基于常规实验室指标的胸腰椎结核临床辅助鉴别诊断模型：一项多中心、回顾性队列研究

刘黔飞[1,2]，阙松年[1,2]，熊南均[1,2]，曾国辉[3]，高琪乐[1,2]，唐明星[1,2]

[1. 中南大学湘雅医院脊柱外科，长沙 410008；2. 老年疾病国家临床医学研究中心(中南大学湘雅医院)，长沙 410008；3. 湘雅博爱康复医院脊柱外科，长沙 410151]

[摘 要] 目的：脊柱结核好发于患者的胸椎和腰椎，但临床上鉴别诊断困难。本研究旨在通过纳入影像学疑似胸椎和腰椎感染的患者，基于常规实验室检查指标，建立一种辅助鉴别胸腰椎结核与非结核脊柱感染的诊断模型。**方法：**连续收集影像学提示胸椎或腰椎感染患者的临床资料。根据最终诊断结果将患者分为胸腰椎结核组和非结核性脊柱感染组。候选变量包括40个临床常规实验室检查变量。首先采用Boruta算法对全部候选变量进行筛选。随后将全部病例按照7:3比例随机分为训练集和验证集，其中70%的病例用于模型构建，30%的病例用于模型验证。在训练集中，对Boruta法筛选出的变量进一步进行Logistic回归分析，筛选具有统计学意义和临床解释价值的独立诊断变量，并基于最终纳入模型的变量构建胸腰椎结核辅助鉴别诊断模型。进一步绘制列线图，将各预测变量对诊断结果的贡献以评分形式进行可视化展示。采用受试者操作特征曲线及曲线下面积评价模型在训练集和验证集中的区分能力，并通过验证集对模型诊断效能进行内部验证。同时，结合校准分析和决策曲线分析评价模型预测结果与实际诊断结果的一致性及其潜在临床净收益。**结果：**共纳入275例胸腰椎感染患者，结核组104例，非结核组171例。采用Boruta法从40个变量中筛选出11个变量：γ干扰素释放试验，结核分枝杆菌抗体，红细胞计数，血红蛋白，淋巴细胞计数，单核细胞百分比，高密度脂蛋白，D-二聚体，C反应蛋白，红细胞沉降率，活化部分凝血活酶时间，并采用Logistic回归建立模型，其中有显著差异的5个变量(高密度脂蛋白、结核抗体、单核细胞百分比、淋巴细胞计数及γ干扰素释放试验)绘制列线图，每个变量均可根据其取值转换为相应评分，各项评分累加后可用于估计患者为胸腰椎结核的预测概率。模型在训练集中表现出较好的区分能力，受试者操作特征曲线下面积为0.877；在验证集中仍保持稳定的诊断效能，受试者操作特征曲线下面积为0.875，提示该模型具有较好的内部验证效果和一定的泛化能力。校准分析显示，模型预测概率与实际诊断结果具有较好一致性。决策曲线分析显示，在一定阈值概率范围内，该模型较单纯假设所有患者均为胸腰椎结核或均为非结核性脊柱感染具有更高的临床净收益，提示其可为临床鉴别诊断提供增量价值。**结论：**5个常规实验室指标(高密度脂蛋白、结核抗体、单核细胞百分比、淋巴细胞计数、γ干扰素释放试验)可用于构建胸腰椎结核辅助鉴别诊断模型。该模型具有显著净收益，具有较好的区分胸腰椎结核与非结核脊柱感染的能力，作为病原学结果回报前的辅助鉴别模型具有潜在应用价值。

[关键词] 胸腰椎结核；诊断模型；辅助诊断；列线图；血清学检验

收稿日期(Date of reception)：2026-03-18

第一作者(First author)：刘黔飞，Email: liu1qf@163.com, ORCID: 0009-0008-2873-3210；阙松年，Email: 13765692937@163.com, ORCID: 0009-0001-0341-5522

通信作者(Corresponding author)：唐明星，副主任医师，Email: 404350@csu.edu.cn, ORCID: 0009-0004-2356-2572

基金项目(Foundation item)：国家自然科学基金(82472469，82072460)；湖南省自然科学基金(2025JJ90279)；中南大学中央高校基本科研业务费专项资金(1053320242324)。This work was supported by the National Natural Science Foundation (82472469, 82072460), the Project of Natural Science Foundation of Hunan Province (2025JJ90279), and the Fundamental Research Funds for the Central Universities of Central South University (1053320242324), China.

开放获取(Open access)：本文遵循知识共享许可协议，允许第三方用户按照署名-非商业性使用-禁止演绎4.0(CC BY-NC-ND 4.0)的方式，在任何媒介以任何形式复制、传播本作品(https://creativecommons.org/licenses/by-nc-nd/4.0/)。

©Journal of Central South University (Medical Science). All rights reserved.

A clinical auxiliary differential diagnostic model for thoracolumbar spinal tuberculosis based on routine laboratory indicators: A multicenter retrospective cohort study

LIU Qianfei[1,2], QUE Songnian[1,2], XIONG Nanjun[1,2], ZENG Guohui[3], GAO Qile[1,2], TANG Mingxing[1,2]

[1. Department of Spine Surgery, Xiangya Hospital, Central South University, Changsha 410008; 2. National Clinical Research Center for Geriatric Disorders (Xiangya Hospital of Central South University), Changsha 410008; 3. Department of Spine Surgery, Xiangya Boai Rehabilitation Hospital, Changsha 410151, China]

ABSTRACT

Objective: Spinal tuberculosis commonly involves the thoracic and lumbar vertebrae, but its clinical differential diagnosis remains challenging. This study included patients with imaging findings suggestive of thoracic or lumbar spinal infection and aims to establish a diagnostic model based on routine laboratory indicators to assist in differentiating thoracolumbar spinal tuberculosis from non-tuberculous spinal infections.

Methods: Clinical data were consecutively collected from patients whose imaging findings suggested thoracic or lumbar spinal infection. Patients were divided into a thoracolumbar spinal tuberculosis group and a non-tuberculous spinal infection group according to the final diagnosis. Candidate variables included 40 routine clinical laboratory indicators. First, the Boruta algorithm was used to screen all candidate variables. All cases were then randomly divided into a training set and a validation set at a ratio of 7∶3, with 70% of cases used for model construction and 30% for model validation. In the training set, the variables selected by the Boruta method were further analyzed using logistic regression to identify independent diagnostic variables with statistical significance and clinical interpretability. An auxiliary differential diagnostic model for thoracolumbar spinal tuberculosis was then constructed based on the final variables included in the model. A nomogram was further developed to visually present the contribution of each predictor to the diagnostic outcome in the form of scores. Receiver operating characteristic curves and the area under the curve were used to evaluate the discriminative ability of the model in the training and validation sets, and the diagnostic performance of the model was internally validated using the validation set. Calibration analysis and decision curve analysis were also performed to evaluate the consistency between predicted probabilities and actual diagnostic results, as well as the potential clinical net benefit of the model.

Results: A total of 275 patients with thoracolumbar spinal infection were included, comprising 104 patients in the tuberculosis group and 171 patients in the non-tuberculous group. The Boruta method selected 11 variables from the 40 candidate variables: Interferon-γ release assay, *Mycobacterium tuberculosis* antibody, red blood cell count, hemoglobin, lymphocyte count, monocyte percentage, high-density lipoprotein, D-dimer, C-reactive protein, erythrocyte sedimentation rate, and activated partial thromboplastin time. A model was then established using Logistic regression. Five variables with significant differences, namely high-density lipoprotein, tuberculosis antibody, monocyte percentage, lymphocyte count, and interferon-γ release assay, were used to construct the nomogram. Each variable

©Journal of Central South University (Medical Science). All rights reserved.

can be converted into a corresponding score according to its value, and the total score can be used to estimate the predicted probability of thoracolumbar spinal tuberculosis. The model showed good discriminative ability in the training set, with an area under the receiver operating characteristic curve of 0.877. It maintained stable diagnostic performance in the validation set, with an area under the curve of 0.875, suggesting good internal validation performance and certain generalizability. Calibration analysis showed good agreement between the predicted probabilities and actual diagnostic results. Decision curve analysis demonstrated that, within a certain range of threshold probabilities, the model provided higher clinical net benefit than the simple assumption that all patients had thoracolumbar spinal tuberculosis or that all patients had non-tuberculous spinal infection, indicating its incremental value for clinical differential diagnosis.

Conclusion: Five routine laboratory indicators, namely high-density lipoprotein, tuberculosis antibody, monocyte percentage, lymphocyte count, and interferon-γ release assay, can be used to construct an auxiliary differential diagnostic model for thoracolumbar spinal tuberculosis. This model has significant net benefit and good ability to distinguish thoracolumbar spinal tuberculosis from non-tuberculous spinal infection. It has potential application value as an auxiliary differential diagnostic model before etiological results become available.

KEY WORDS thoracolumbar spinal tuberculosis; diagnostic model; auxiliary diagnosis; nomogram; serological test

结核病是全球十大死亡原因之一[1]，根据世界卫生组织[2]报道，2023年全球共有820万人新诊断出结核病，125万人因病死亡。肺外结核病占结核病例的10%，脊柱是最常见的受累部位，脊柱结核(spinal tuberculosis，STB)约占骨结核病例的50%[3-4]，胸椎和腰椎是最容易发生STB的部位[5]，其病理特征为活动性骨质破坏，并导致骨小梁微结构改变[6-7]，临床表现包括腰背痛、低热、脊柱后凸(椎体破坏导致)、硬膜外寒性脓肿及死骨形成等，最终导致脊髓受压和神经系统后遗症[8]。

目前，STB的确诊仍高度依赖病原学或病理学证据。传统培养虽为直接证据，但存在耗时长、阳性率有限、易受既往治疗影响等局限[9]。近年来，结核分枝杆菌及利福平耐药基因检测(*Mycobacterium tuberculosis* and rifampicin resistance gene detection，Xpert MTB/RIF)及宏基因组下一代测序(metagenomic next-generation sequencing，mNGS)等分子快速检测技术显著提高了结核分枝杆菌及利福平耐药的快速检出能力，被推荐用于多种肺外结核标本的初始检测[10]。在STB中，Xpert MTB/RIF对开放活体组织检查(以下简称“活检”)及CT引导穿刺活检标本也显示出较高的诊断准确性[11]。尽管如此，这类技术仍依赖病灶穿刺或术中取材。尚缺少一种低侵袭、低成本且便于推广的辅助鉴别工具，以满足在术前或病原学结果回报前对患者进行快速初筛和风险分层的需求[12]。血清学指标是患者入院后第一手资料，多种常规血液学和宿主反应相关生物标志物在STB诊断中具有潜在价值[13]，如何将这些分散的信号整合为稳定、可解释、可推广的辅助鉴别工具，仍是当前临床转化中的关键问题。

机器学习及现代临床鉴别诊断模型为多指标整合提供了可行路径[14]。研究[15]表明，基于机器学习或多变量建模的方法可用于结核与其他感染性疾病的鉴别诊断。相较于依赖单一指标的判断，机器学习辅助的特征筛选能够从多维数据中识别与结局最相关的变量，而结合Logistic回归和列线图则能够在保持模型可解释性的同时提升临床可用性[16]。利用机器学习系统整合血清学差异可有助于建立病原学结果回报前的辅助诊断模型。

本研究旨在通过收集胸腰椎感染患者的常规血清学指标，使用Boruta法筛选变量，采用Logistic回归建立一种辅助诊断模型并验证诊断性能，在病原学结果回报前辅助鉴别胸腰椎结核与非结核脊柱感染。

©Journal of Central South University (Medical Science). All rights reserved.

1 资料与方法

1.1 伦理声明

本研究已获得中南大学湘雅医院医学伦理审查委员会批准(审批号：202212775)。

1.2 纳入、排除及诊断标准

本研究是一项多中心、回顾性观察性队列研究，选取2019年1月至2024年10月于中南大学湘雅医院、湘雅博爱康复医院、湖南省胸科医院、长沙市第一医院及贵阳市第一人民医院就诊的胸腰椎感染患者。该队列包括临床、影像学及微生物学数据，获取并分析患者入院时第1次血清学检验结果。纳入标准：1)影像学结果显示疑似胸椎或腰椎感染；2)有完整的临床检查资料，通过开放手术或穿刺活检获得病灶组织标本并明确了病原菌类型。排除标准：1)合并自身免疫性疾病或人类免疫缺陷病毒感染；2)多部位感染或脊柱术后感染；3)脊柱肿瘤。胸腰椎结核诊断标准：1)病灶标本培养出结核分枝杆菌或mNGS/Xpert MTB/RIF检测出结核分枝杆菌；2)病理检查提示结核菌感染且抗结核治疗有效。非结核脊柱感染诊断标准：1)病灶标本培养或mNGS检测提示结核分枝杆菌以外的病原微生物；2)病理学检查不支持结核菌感染且抗感染治疗有效。

1.3 纳入的主要变量

收集患者的性别、年龄及入院后第1次常规血清学检验结果，包括结核分枝杆菌抗体(*Mycobacterium tuberculosis* antibody，TB-antibody)、γ干扰素释放试验(interferon-gamma release assays，IGRAs)、白细胞(white blood cell count，WBC)、红细胞(red blood cell count，RBC)、血红蛋白(hemoglobin，HGB)、血小板(platelet count，PLT)、中性粒细胞(neutrophil count，Neut)、淋巴细胞(lymphocyte count，Lymph)、嗜酸性粒细胞(eosinophil count，EO)、嗜碱性粒细胞(basophil count，BASO)、单核细胞(monocyte count，Mono)、中性粒细胞百分比(neutrophil percentage，Neut%)、淋巴细胞百分比(lymphocyte percentage，Lymph%)、嗜碱性粒细胞百分比(basophil percentage，BASO%)、嗜酸性粒细胞百分比(eosinophil percentage，EO%)、单核细胞百分比(monocyte percentage，Mono%)、红细胞分布宽度(red cell distribution width，RDW)、血小板压积(plateletcrit，PCT)、平均血小板体积(mean platelet volume，MPV)、总蛋白(total protein，TP)、白蛋白(albumin，A)、球蛋白(globulin，G)、白蛋白/球蛋白(albumin-to-globulin ratio，A/G)、丙氨酸氨基转移酶(alanine aminotransferase，ALT)、天冬氨酸氨基转移酶(aspartate transferase，AST)、血尿素氮(blood urea nitrogen，BUN)、肌酐(creatinine，Cr)、甘油三酯(triglycerides，TG)、胆固醇(total cholesterol，Chol)、高密度脂蛋白(high-density lipoprotein cholesterol，HDL)、低密度脂蛋白(low-density lipoprotein cholesterol，LDL)、血糖(blood glucose，BS)、凝血酶原时间(prothrombin time，PT)、活化部分凝血活酶时间(activated partial thromboplastin time，APTT)、国际标准化比值(international normalized ratio，INR)、D-二聚体(D-dimer，DD)、红细胞沉降率(erythrocyte sedimentation rate，ESR)及C反应蛋白(C-reactive protein，CRP)。所有患者的术中标本均行细菌培养、mNGS或多重PCR等分子诊断，明确感染病原菌类型，并依此进行分类。

1.4 统计学处理

采用R语言4.4.2版本进行数据分析。符合正态分布的计量资料以均数±标准差表示，2组之间比较采用t检验；不符合正态分布的计量资料以中位数(第1四分位数，第3四分位数)表示，采用Mann-Whitney U检验；计数资料以频数(构成比)表示，采用χ^2检验或Fisher精确检验。P<0.05为差异具有统计学意义。

受试者操作特征(receiver operating characteristic，ROC)曲线作为模型的评价指标。使用相关性热图观察各变量间的联系。使用诊断模型校准曲线判断模型与实际情况的一致性。使用决策曲线分析(decision curve analysis，DCA)评价模型的临床效益。模型开发使用Logistic回归模型。在完成数据预处理后，使用caret包中的createDataPartition函数，按照结局变量分组进行分层抽样，将数据划分为70%训练集和30%验证集；随机种子设为3 456，以保证结果可重复。模型输入变量均采集自患者入院时首次常规实验室检查结果，最终病原学/病理学诊断仅用于研究中的结局定义与模型标签标注。

2 结　果

2.1 患者基本特征

根据确立的纳排标准，共纳入275例疑似胸腰椎感染患者。根据诊断标准，结核的患者104例，非结核感染的患者171例。2组患者的临床特征、常规实验室数据和这些指标的统计学比较结果(表1)显示，2组在年龄、性别及糖尿病等基础疾病患病率方面差

©Journal of Central South University (Medical Science). All rights reserved.

异均无统计学意义(均P>0.05)；而在IGRAs、TB-antibody、RBC、HGB、Lymph、Mono%、HDL、PT、APTT、INR、ESR、DD、WBC、PLT、Mono、A、A/G、LDL、CRP的差异均具有统计学意义(均P<0.05)。

表1 脊柱感染患者的基本资料及常规实验室数据比较

Table 1 Comparative analysis of routine laboratory parameters in patients with spinal infections

变量	总人数(n=275)	非胸腰椎结核(n=171)	胸腰椎结核(n=104)	$\chi^2/t/U$	P
性别/[例(%)]				0.027	0.869
女性	130(47)	82(48)	48(46)		
男性	145(53)	89(52)	56(54)		
年龄/岁	59(51, 68)	59(52, 67)	60(51, 69)	8 522.500	0.564
糖尿病/[例(%)]	12(4.4)	8(4.7)	4(3.8)	0.743	1.000
高血压/[例(%)]	25(9.1)	16(9.4)	9(8.7)	0.844	1.000
肺结核/[例(%)]	5(1.8)	2(1.2)	3(2.9)	0.302	0.369
长期免疫抑制剂使用史/[例(%)]	3(1.1)	2(1.2)	0(0)	0.026	0.528
肝功能异常/[例(%)]	4(1.5)	2(1.2)	2(2.0)	0.613	0.634
肾功能异常/[例(%)]	1(0.4)	1(0.6)	0(0)	0.435	1.000
IGRAs/[例(%)]				70.679	<0.001
阴性	156(57)	131(77)	25(24)		
阳性	119(43)	40(23)	79(76)		
TB-antibody/[例(%)]				27.405	<0.001
阴性	234(85)	161(94)	73(70)		
阳性	41(15)	10(6)	31(30)		
WBC/($10^9\cdot L^{-1}$)	6.50(4.88, 8.30)	6.80(5.22, 8.61)	6.10(4.71, 7.58)	10 505.500	0.012
RBC/($10^{12}\cdot L^{-1}$)	3.94±0.64	3.81±0.60	4.14±0.64	−4.285	<0.001
HGB/($g\cdot L^{-1}$)	114.36±17.96	110.75±17.53	120.30±17.13	−4.441	<0.001
PLT/($10^9\cdot L^{-1}$)	266.00(200.00, 324.50)	276.00(207.00, 330.50)	243.00(193.75, 305.75)	10 252.000	0.034
Neut/($10^9\cdot L^{-1}$)	4.34(2.94, 6.02)	4.50(2.91, 6.50)	4.13(3.00, 5.50)	9 709.000	0.202
Lymph/($10^9\cdot L^{-1}$)	1.31(1.00 1.71)	1.40(1.08, 1.88)	1.13(0.90, 1.50)	11 063.000	<0.001
EO/($10^9\cdot L^{-1}$)	0.10(0.05, 0.20)	0.10(0.04, 0.20)	0.11(0.06, 0.20)	8 007.000	0.166
BASO/($10^9\cdot L^{-1}$)	0.02(0.01, 0.04)	0.03(0.01, 0.04)	0.02(0.01, 0.03)	9 594.000	0.266
Mono/($10^9\cdot L^{-1}$)	0.50(0.39, 0.65)	0.47(0.36, 0.60)	0.50(0.40, 0.70)	7 578.000	0.039
Neut%	68.60(59.75, 75.30)	67.90(58.30, 76.60)	68.95(63.00, 73.42)	8 901.500	0.989
Lymph%	20.20(15.25, 27.55)	21.70(15.00, 29.10)	19.35(15.38, 22.57)	9 779.500	0.165
BASO%	0.40(0.30, 0.65)	0.40(0.20, 0.70)	0.45(0.30, 0.60)	8 127.500	0.229
EO%	1.50(0.60, 3.00)	1.4(0.50, 2.60)	1.75(0.80, 3.20)	7 911.500	0.125
Mono%	7.40(5.90, 9.30)	6.7(5.40, 8.85)	8.45(6.70, 10.00)	5 917.000	<0.001
RDW	13.70(12.70, 14.75)	13.80(12.70, 14.80)	13.60(12.70, 14.62)	9 299.000	0.525
PCT/($10^9\cdot L^{-1}$)	0.23(0.18, 0.30)	0.24(0.18, 0.31)	0.23(0.19, 0.28)	9 375.000	0.450
MPV/fL	9.00(8.10, 10.10)	9.00(8.06, 10.05)	9.00(8.10, 10.10)	8 783.500	0.866
TP/($g\cdot L^{-1}$)	69.70(65.15, 73.75)	69.20(64.95, 73.75)	70.05(65.47, 73.38)	8 619.000	0.670
A/($g\cdot L^{-1}$)	37.30±4.95	36.59±5.21	38.46±4.27	−3.226	0.001
G/($g\cdot L^{-1}$)	31.20(28.20, 35.40)	31.40(28.55, 36.25)	30.60(27.60, 34.85)	9 904.500	0.114
A/G	1.21±0.29	1.17±0.30	1.27±0.27	−2.981	0.003
ALT/($U\cdot L^{-1}$)	18.60(11.55, 31.10)	19.00(11.70, 33.05)	17.70(11.43, 27.77)	9 518.000	0.328
AST/($U\cdot L^{-1}$)	20.60(16.10, 28.85)	19.90(15.65, 29.05)	22.20(17.20, 28.50)	7 987.000	0.157

©Journal of Central South University (Medical Science). All rights reserved.

表1(续)

变量	总人数(n=275)	非胸腰椎结核(n=171)	胸腰椎结核(n=104)	$\chi^2/t/U$	P
BUN/(mmol·L^{-1})	5.38(4.20, 6.64)	5.54(4.12, 6.83)	5.10(4.26, 6.31)	9 417.500	0.412
Cr/(mmol·L^{-1})	65.10(52.40, 79.00)	65.00(52.00, 80.70)	65.55(54.22, 76.38)	8 842.500	0.939
TG/(mmol·L^{-1})	1.27(1.02, 1.65)	1.34(1.06, 1.69)	1.17(0.99, 1.56)	9 974.000	0.091
Chol/(mmol·L^{-1})	4.50(3.90, 5.10)	4.48(3.80, 4.98)	4.54(4.07, 5.24)	7 849.500	0.103
HDL/(mmol·L^{-1})	1.08(0.90, 1.31)	1.00(0.84, 1.21)	1.18(1.04, 1.39)	5 542.000	<0.001
LDL/(mmol·L^{-1})	3.02(2.58, 3.58)	2.95(2.55, 3.43)	3.14(2.64, 3.77)	7 579.500	0.040
BS/(mmol·L^{-1})	5.34(4.81, 6.38)	5.42(4.09, 6.40)	5.16(4.73, 6.31)	9 999.000	0.084
PT/s	12.10(11.30, 12.90)	12.30(11.45, 13.30)	11.70(11.17, 12.33)	11 358.500	<0.001
APTT/s	30.50(26.85, 36.85)	32.00(27.55, 37.50)	28.30(25.30, 33.05)	11 466.000	<0.001
INR	0.98(0.93, 1.06)	1.00(0.95, 1.07)	0.96(0.91, 1.03)	11 171.500	<0.001
DD/(mg·L^{-1})	0.36(0.21, 0.78)	0.45(0.22, 1.06)	0.28(0.19, 0.51)	11 054.000	<0.001
ESR/(mm·h^{-1})	79.00(40.00, 110.00)	90.00(47.00, 117.50)	64.00(33.75, 93.50)	11 279.000	<0.001
CRP/(mg·L^{-1})	24.19(7.68, 53.92)	28.50(7.55, 72.43)	19.01(7.94, 41.31)	10 165.000	0.047

符合正态分布的计量资料以均数±标准差表示，2组之间比较采用t检验；不符合正态分布的计量资料以中位数(第1四分位数，第3四分位数)表示，采用Mann-Whitney U检验；计数资料以频数(构成比)表示，采用χ^2检验或Fisher精确概率法。TB：结核分枝杆菌；IGRAs：γ干扰素释放试验；WBC：白细胞；RBC：红细胞；HGB：血红蛋白；PLT：血小板；Neut：中性粒细胞；Lymph：淋巴细胞；EO：嗜酸性粒细胞；BASO：嗜碱性粒细胞；Mono：单核细胞；Neut%：中性粒细胞百分比；Lymph%：淋巴细胞百分比；BASO%：嗜碱性粒细胞百分比；EO%：嗜酸性粒细胞百分比；Mono%：单核细胞百分比；RDW：红细胞分布宽度；PCT：血小板压积；MPV：平均血小板体积；TP：总蛋白；A：白蛋白；G：球蛋白；A/G：白蛋白/球蛋白；ALT：丙氨酸氨基转移酶；AST：天冬氨酸氨基转移酶；BUN：血尿素氮；Cr：肌酐；TG：甘油三酯；Chol：胆固醇；HDL：高密度脂蛋白；LDL：低密度脂蛋白；BS：血糖；PT：凝血酶原时间；APTT：活化部分凝血活酶时间；INR：国际标准化比值；DD：D-二聚体；ESR：红细胞沉降率；CRP：C反应蛋白。

2.2 单因素分析常规实验室指标在2组之间的差异

根据单因素分析结果表明，IGRAs具有最好的诊断有效性，AUC为0.763；HDL、Mono%、HGB、RBC、APTT、PT、ESR、INR、Lymph、DD、TB-antibody、A的AUC值为0.6~0.7，具有一定的诊断价值，但需要进一步评估并筛选(图1)。

2.3 Boruta法筛选变量

相关性热图显示部分变量之间存在很强的相关性(图2A)。使用Boruta法筛选所统计的40个变量，根据Z值排序，并确定11个与TTB密切相关的指标用于后续诊断模型拟合，包括IGRAs、TB-antibody、RBC、HGB、Lymph、Mono%、HDL、DD、CRP、APTT和ESR(图2B)。

2.4 胸腰椎STB的辅助诊断模型建立

基于结局变量进行分层抽样，将患者分为验证集与训练集，患者基本资料和数据见表2。将Boruta筛选得到的候选变量同时纳入Logistic回归初始模型获得单变量P值，并基于全变量Logistic回归模型进一步进行逐步回归分析，结果显示，与全变量模型相比，逐步筛选直至模型仅剩HDL、Mono%、Lymph、IGRAs及TB-antibody 5个参数后，模型的AIC值由200.00降低至168.89，为最优AIC值。进一步分析简化模型的多重共线性，结果显示，最终Logistic回归模型中各变量的方差膨胀因子均较低，VIF值范围为1.059~1.159(表3)，均明显低于常用阈值5，提示模型中不存在明显多重共线性。因此最终选定HDL、Mono%、Lymph、IGRAs及TB-antibody共5个参数构建辅助诊断模型，并根据Logistic诊断模型绘制列线图(图3)，可用于临床病原学结果回报前辅助鉴别结核和非结核感染。将患者对应的5个变量信息投影在列线图上，所得分数总和即为患者所患病原菌为结核分枝杆菌的概率。

©Journal of Central South University (Medical Science). All rights reserved.

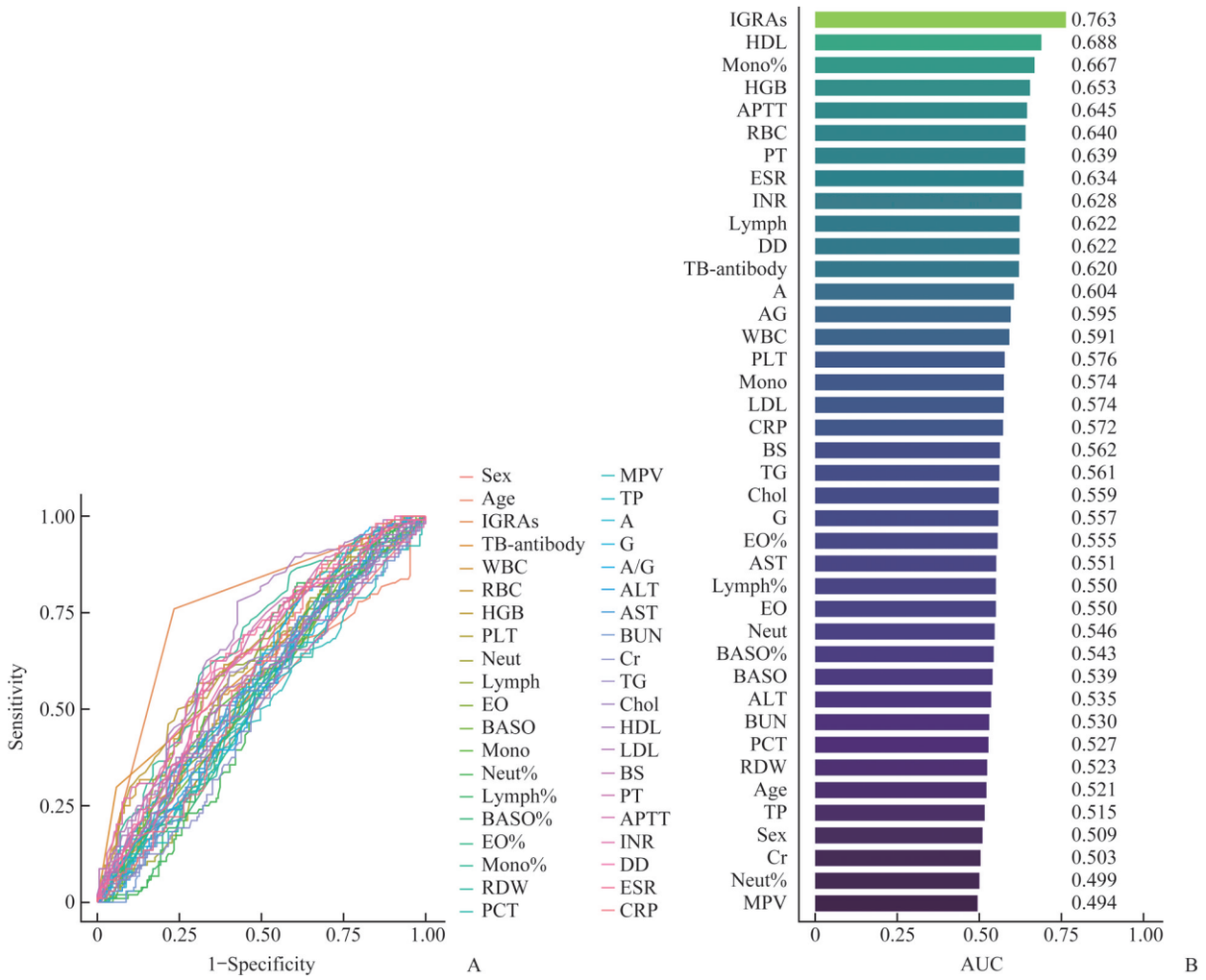


图1 血清学变量单因素分析结果

Figure 1 Univariate analysis results of serological variables

A: Receiver operating characteristic curves for all variables. B: Ranking of area under the curve values among all candidate variables. TB-antibody: *Mycobacterium tuberculosis* antibody; WBC: White blood cell count; RBC: Red blood cell count; HGB: Hemoglobin; PLT: Platelet count; Neut: Neutrophil count; Lymph: Lymphocyte count; EO: Eosinophil count; BASO: Basophil count; Mono: Monocyte count; Neut%: Neutrophil percentage; Lymph%: Lymphocyte percentage; BASO%: Basophil percentage; EO%: Eosinophil percentage; Mono%: Monocyte percentage; RDW: Red cell distribution width; PCT: Plateletcrit; MPV: Mean platelet volume; TP: Total protein; A: Albumin; G: Globulin; A/G: Albumin-to-globulin ratio; ALT: Alanine aminotransferase; AST: Aspartate transferase; BUN: Blood urea nitrogen; Cr: Creatinine; TG: Triglycerides; Chol: Total cholesterol; HDL: High-density lipoprotein cholesterol; LDL: Low-density lipoprotein cholesterol; BS: Blood glucose; PT: Prothrombin time; APTT: Activated partial thromboplastin time; INR: International normalized ratio; DD: D-dimer; ESR: Erythrocyte sedimentation rate; CRP: C-reactive protein; ROC: Receiver operating characteristic; AUC: Area under the characteristic curve.

2.5 评估TTB辅助诊断模型的诊断效能

绘制训练集的ROC曲线，其AUC为0.877(图4A)；使用验证集进一步评估模型的诊断性能，绘制验证集ROC曲线，AUC为0.875(图4B)。使用验证集绘制模型的校准曲线，并采用1 000次bootstrap进行内部校正，结果显示，该模型的平均绝对误差(mean absolute error，MAE)为0.025，提示鉴别概率与实际观察概率之间具有较好一致性(图4C)。进一步评估模型的临床效益，绘制DCA曲线，结果表明，在较宽的阈值概率范围内，训练集和验证集的模型曲线均高于“treat none”策略，且在大部分阈值范围内高于“treat all”策略(图4D)，提示该模型在临床决策中可获得正向净获益，具有潜在临床应用价值。

©Journal of Central South University (Medical Science). All rights reserved.

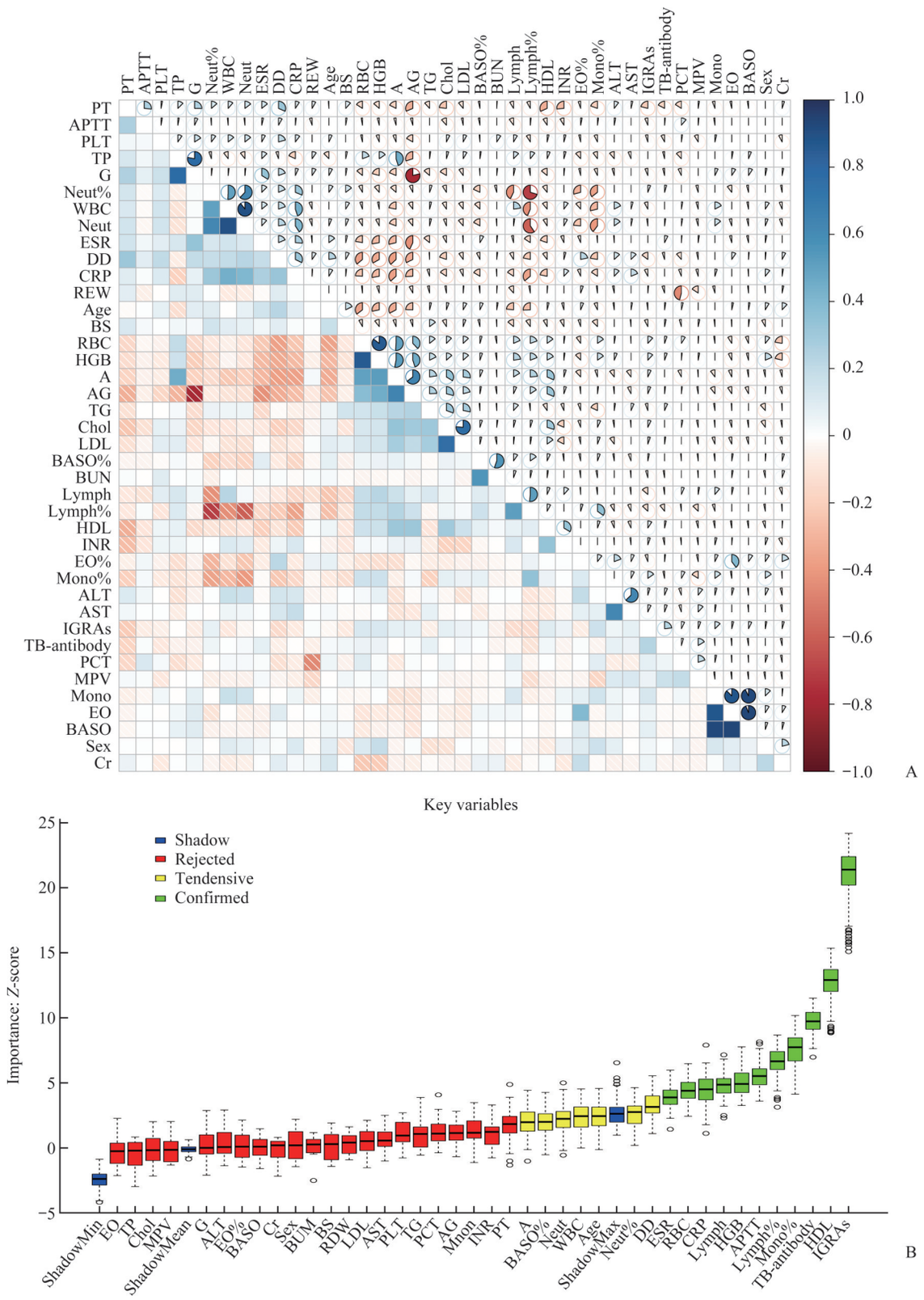


图2　变量间相关性热图及 Boruta 法筛选变量

Figure 2　Correlation heatmap of variables and variable selection using the Boruta method

A: Correlation heatmap showing interrelationships between multiple variables. B: Boruta method screening 11 variables from 40 candidates.

©Journal of Central South University (Medical Science). All rights reserved.

表2 训练集与验证集患者的基本资料及常规实验室数据比较

Table 2 Comparison of baseline characteristics and routine laboratory parameters between the training and validation cohorts

变量	总人数(n=275)	验证集(n=82)	训练集(n=193)	$\chi^2/t/U$	P
性别/[例(%)]				0.038	0.846
女性	130(47)	40(49)	90(47)		
男性	145(53)	42(51)	103(53)		
年龄/岁	59(51, 68)	59(51, 68)	59(51, 68)	7 848.500	0.915
IGRAs/[例(%)]				0	1.000
阴性	156(57)	47(57)	109(56)		
阳性	119(43)	35(43)	84(44)		
TB-antibody/[例(%)]				0	1.000
阴性	234(85)	70(85)	164(85)		
阳性	41(15)	12(15)	29(15)		
RBC/($10^{12}\cdot L^{-1}$)	3.94±0.64	3.95±0.60	3.93±0.65	0.183	0.855
HGB/($g\cdot L^{-1}$)	114.36±17.96	114.79±18.91	114.18±17.58	0.250	0.803
Lymph/($10^{9}\cdot L^{-1}$)	1.31(1.00, 1.71)	1.20(1.00, 1.69)	1.34(0.98, 1.71)	7 606.500	0.612
Mono%	7.40(5.90, 9.30)	7.60(5.82, 9.45)	7.30(5.90, 9.10)	7 799.000	0.968
A/($g\cdot L^{-1}$)	37.30±4.95	37.63±5.23	37.16±4.83	0.694	0.489
HDL/($mmol\cdot L^{-1}$)	1.08(0.90, 1.31)	1.04(0.87, 1.26)	1.11(0.92, 1.33)	7 234.000	0.261
PT/s	12.10(11.30, 12.90)	12.10(11.43, 13.30)	12.20(11.30, 12.80)	8 204.500	0.629
APTT/s	30.5(26.85, 36.85)	30(26.52, 37.22)	30.6(27.1, 36.5)	7 605.000	0.610
DD/($mg\cdot L^{-1}$)	0.36(0.21, 0.78)	0.36(0.21, 0.66)	0.36(0.21, 0.79)	7 425.000	0.419

符合正态分布的计量资料以均数±标准差表示，2组之间比较采用t检验；不符合正态分布的计量资料以中位数(第1四分位数，第3四分位数)表示，采用Mann-Whitney U检验；计数资料以频数(构成比)表示，采用χ^2检验或Fisher精确概率法。

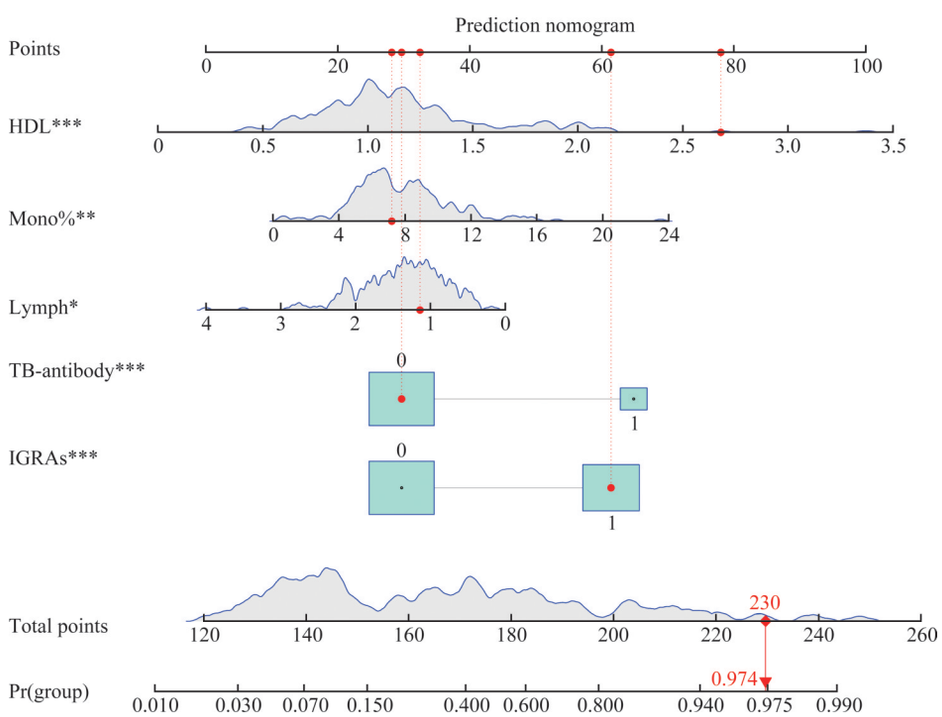


图3 胸腰椎结核辅助鉴别的列线图诊断模型

Figure 3 Nomogram-based diagnostic model for the auxiliary differential diagnosis of thoracolumbar tuberculosis

Red dots indicate the values of an example patient for each predictor. The connecting lines illustrate the points assigned to each variable and the mapping of the total points to the predicted probability of thoracolumbar spinal tuberculosis. *P<0.05, **P<0.01, ***P<0.001.

©Journal of Central South University (Medical Science). All rights reserved.

表3　构建Logistic回归模型的变量的VIF值

Table 3　VIF values of variables in the Logistic regression model

变量	VIF值
IGRAs	1.159
TB-antibody	1.123
Lymph	1.128
Mono%	1.059
HDL	1.142

VIF：方差膨胀因子。

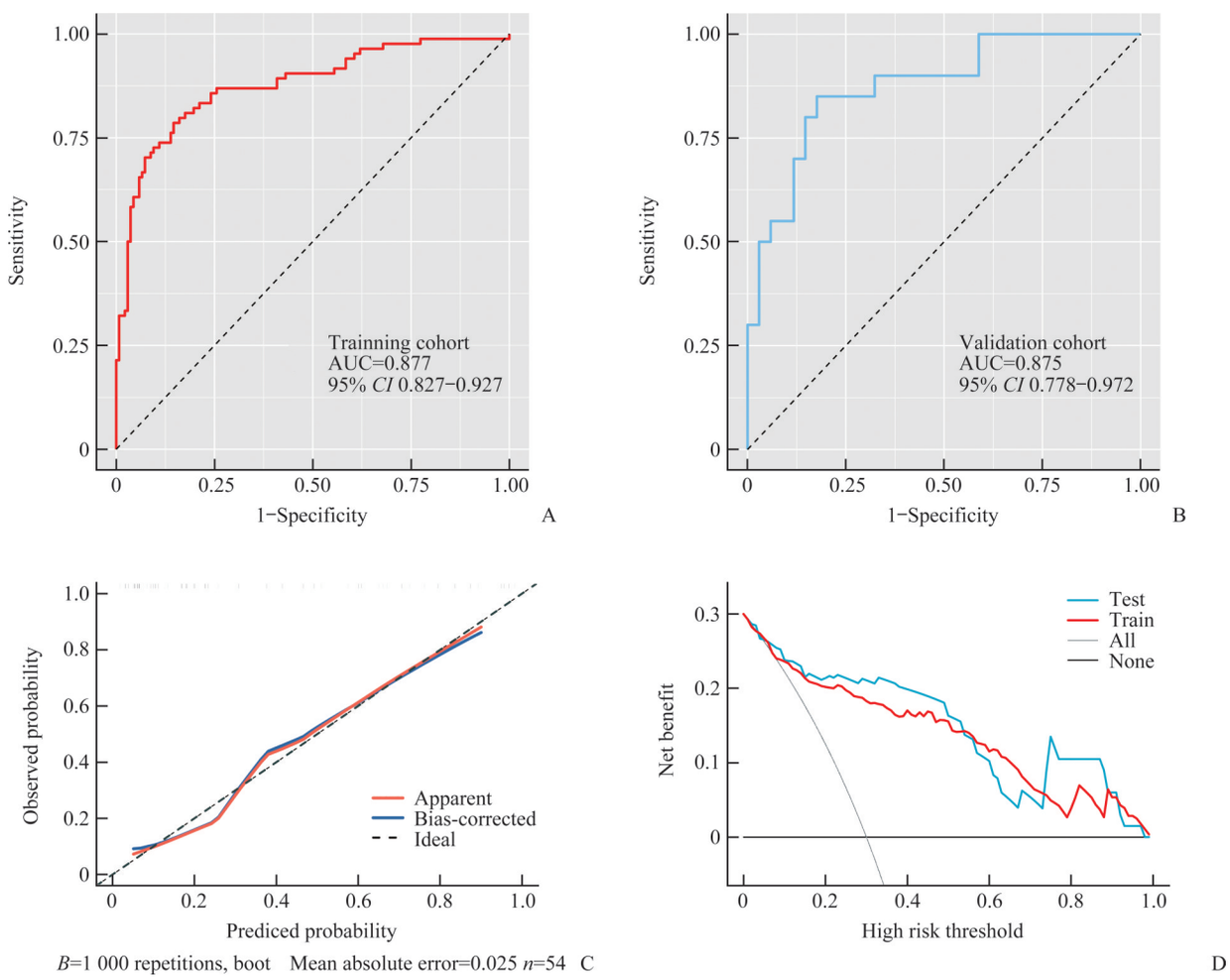


图4　列线图评估临床辅助诊断模型

Figure 4　Nomogram evaluation of clinical adjunctive diagnostic model

A: ROC curve of training cohort model. B: ROC curve of validation cohort model. C: Calibration curve of testing cohort model. D: DCA curve of Logistic diagnostic model. ROC: Receiver operating characteristic; AUC: Area under the curve; DCA: Decision curve analysis.

3　讨　论

本研究在多家医院回顾性地收集了275位胸腰椎感染患者的临床数据。根据最终病原学/病理学诊断结果将患者分为结核组及非结核感染组，将2组血清学数据进行对比发现IGRAs、TB-antibody、RBC、HGB、Lymph、Mono%、HDL、LDL等数据存在显著差异，并基于Boruta法及Logistic回归模型构建筛

©Journal of Central South University (Medical Science). All rights reserved.

选并验证了HDL、Mono%、Lymph、IGRAs、TB-antibody共5个血清学指标是胸腰椎结核患者的核心鉴别诊断因素。

在椎体破坏性疾病的临床诊疗中，STB与非结核性脊柱感染常表现出高度重叠的症状学和影像学特征，均可出现腰背痛、炎症反应升高及椎体破坏[17]，导致病原学结果回报前的鉴别诊断尤为困难[18]。这种不确定性不仅影响经验性抗感染方案的选择，也直接关系到术前评估、取材策略及后续治疗路径的制订。因此，构建一种在病原学结果明确前提供辅助判断的鉴别工具，具有明确的临床现实意义。本研究在既往研究[15, 19]的基础上，进一步将研究对象限定为影像学疑似胸腰椎感染患者，并排除了脊柱肿瘤、脊柱术后感染及多部位感染等干扰因素，构建了一个更具针对性和实用性的辅助鉴别模型。与此同时，笔者采用Boruta方法进行变量初筛，并结合Logistic回归构建列线图，在保留模型可解释性的前提下，实现了多项常规血清学指标的整合分析[20-21]。

在筛选出的指标中，IGRAs具有一定的临床解释性。IGRAs通过结核分枝杆菌特异性抗原刺激T细胞，检测γ干扰素释放水平，可反映机体对结核分枝杆菌的细胞免疫应答能力[22]。γ干扰素不仅参与单核-巨噬细胞活化和吞噬体成熟，还与宿主抗结核防御密切相关[23-24]。因此，IGRAs进入最终模型具有明确的生物学合理性，也提示在胸腰椎感染的临床鉴别中，宿主对结核分枝杆菌的特异性免疫应答仍是重要的信息来源之一。除IGRAs外，HDL是另一个值得重视的指标。既往研究[25]提示脂质代谢与结核感染关系密切，结核状态下宿主脂质谱会发生重塑。研究发现，HDL水平与肺结核风险呈正相关[26]，HDL功能可能在炎症状态下发生改变，从而影响宿主免疫反应[27-28]。HDL被稳定纳入最终模型，并提示较高HDL水平与胸腰椎结核相关，这表明脂质代谢异常不仅存在于肺结核，也可能参与胸腰椎结核的宿主反应过程。与传统炎症指标相比，HDL的纳入拓展了胸腰椎结核辅助鉴别的指标维度，脂质代谢在胸腰椎结核相关内环境紊乱中具有潜在研究价值。Mono%、Lymph和TB-antibody进入最终模型，同样具有较强的免疫学解释基础。淋巴细胞在抗结核免疫中发挥核心作用，Th1细胞是γ干扰素的重要来源，$CD8^+$T细胞则参与清除感染细胞[29]。B细胞通过抗原呈递激活$CD4^+$T细胞，并在免疫应答过程中提供辅助信号[30]；B细胞及其抗体在抗结核免疫中的作用也受到越来越多关注[31-32]。总之，本研究最终保留的5个变量共同反映了宿主针对结核分枝杆菌的特异性免疫应答、炎症细胞构成变化及代谢状态改变。联合多指标的鉴别模型可多角度显示胸腰椎结核与非结核感染间的内环境状态差异。

在纳入的患者中，病灶培养阳性率(26.21%)较低，与既往报道[33]相近。这可能与脊柱病灶细菌负荷较低及术前抗菌药物使用有关[34-35]。为提高病原学结局判定的准确性，所有入组患者均接受了mNGS或Xpert MTB/RIF检测，并结合病理学结果和随访治疗反应进行分组。近年来，mNGS及Xpert MTB/RIF在脊柱感染中的应用价值已逐渐得到证实，尤其在低菌量、培养阴性的病例中具有补充意义[36-37]。这也保证了结局标签的相对可靠性。

本研究仍存在若干局限性。首先，辅助鉴别模型是在最终确诊队列中建立的。尽管模型所使用的变量均来源于患者入院后的首次常规实验室检查结果，但研究对象均已获得最终病原学/病理学诊断，因此属于在确诊队列中开发和验证的辅助鉴别模型，尚未在真实未确诊场景中完成验证。仍需进一步开展前瞻性研究和外部验证。其次，纳入的患者中糖尿病与高血压患病率低于一般人群，也低于STB中报道的9.2%与11.8%[38]，本研究基于患者入院时病历中记录的明确既往史进行统计，可能遗漏部分未被识别且未被记录的病例，样本代表性和外部推广性仍需谨慎解读。此外，尽管内部验证结果较好，但尚缺乏外部验证队列，模型在不同地区、不同医院及更广泛临床人群中的稳定性和泛化能力仍需进一步确认。

总体而言，本研究表明，基于HDL、Mono%、Lymph、IGRAs和TB-antibody的联合模型能够较好地区分胸腰椎结核与非结核脊柱感染，可为病原学结果回报前的临床辅助鉴别提供参考。未来仍需在更大样本、多中心外部队列中进一步验证其应用价值。

志谢：感谢中南大学湘雅医院、湘雅博爱康复医院、湖南省胸科医院、长沙市第一医院及贵阳市第一人民医院脊柱外科全体医护人员的支持。

作者贡献声明：刘黔飞 数据分析，论文设计与修改；阙松年 论文撰写与修改；熊南均 数据采集；曾国辉 论文指导，经费获取；高琪乐、唐明星 论文设计与指导。所有作者阅读并同意最终的文本。

利益冲突声明：作者声称无任何利益冲突。

参考文献

[1] Suárez I, Fünger SM, Kröger S, et al. The diagnosis and

©Journal of Central South University (Medical Science). All rights reserved.

treatment of tuberculosis[J]. Deutsches Ärzteblatt Int, 2019: 116(43): 729-735. https://doi.org/10.3238/arztebl.2019.0729.

[2] World Health Organization. Global tuberculosis report 2024 [R]. World Health Organization, 2024.

[3] Heyde CE, Lübbert C, Wendt S, et al. Spinal tuberculosis[J]. Z Orthop Unfall, 2022, 160(1): 74-83. https://doi. org/10.1055/a-1285-4994.

[4] Carabalí-Isajar ML, Rodríguez-Bejarano OH, Amado T, et al. Clinical manifestations and immune response to tuberculosis [J]. World J Microbiol Biotechnol, 2023, 39(8): 206. https://doi.org/10.1007/s11274-023-03636-x.

[5] Pourbaix A, Zarrouk V, Allaham W, et al. More complications in cervical than in non-cervical spine tuberculosis[J]. Infect Dis, 2020, 52(3): 170-176. https://doi.org/10.1080/23744235.2019.1690675.

[6] Dunn RN, Ben Husien M. Spinal tuberculosis: review of current management[J]. Bone Joint J, 2018, 100-B(4): 425-431. https://doi.org/10.1302/0301-620x.100b4.bjj-2017-1040.r1.

[7] 陈俊宝, 罗翼, 熊南均, 等. 脊柱结核分枝杆菌感染早期椎体骨小梁微结构及骨密度变化的研究[J]. 中国感染控制杂志, 2024, 23(8): 1001-1006. https://doi.org/10.12138/j.issn.1671-9638.20246239.
CHEN Junbao, LUO Yi, XIONG Nanjun, et al. Changes in the microstructure and bone mineral density of vertebral trabecular bone in the early stages of spinal *Mycobacterium tuberculosis* infection [J]. Chinese Journal of Infection Control, 2024, 23(8): 1001-1006. https://doi.org/10.12138/j.issn.1671-9638.20246239.

[8] Kilborn T, Janse van Rensburg P, Candy S. Pediatric and adult spinal tuberculosis: imaging and pathophysiology[J]. Neuroimaging Clin N Am, 2015, 25(2): 209-231. https://doi.org/10.1016/j.nic.2015.01.002.

[9] Chakravorty S, Simmons AM, Rowneki M, et al. The new xpert MTB/RIF ultra: improving detection of *Mycobacterium tuberculosis*and resistance to rifampin in an assay suitable for point-of-care testing[J/OL]. mBio, 2017, 8(4): e00812-e00817 [2025-12-30]. https://doi.org/10.1128/mbio.00812-17.

[10] Li Y, Yao XW, Tang L, et al. Diagnostic efficiency of metagenomic next-generation sequencing for suspected spinal tuberculosis in China: a multicenter prospective study[J]. Front Microbiol, 2022, 13: 1018938. https://doi.org/10.3389/fmicb.2022.1018938.

[11] Waters R, Laubscher M, Dunn RN, et al. Higher sensitivity of xpert MTB/RIF ultra over tuberculosis culture for the diagnosis of spinal tuberculosis with open or computed tomography-guided biopsies[J]. Open Forum Infect Dis, 2024, 11(1): ofad621. https://doi.org/10.1093/ofid/ofad621.

[12] Leowattana W, Leowattana P, Leowattana T. Tuberculosis of the spine[J]. World J Orthop, 2023, 14(5): 275-293. https://doi.org/10.5312/wjo.v14.i5.275.

[13] Kasule GW, Hermans S, Semugenze D, et al. Non-sputum-based samples and biomarkers for detection of *Mycobacterium tuberculosis*: the hope to improve childhood and HIV-associated tuberculosis diagnosis[J]. Eur J Med Res, 2024, 29 (1): 502. https://doi.org/10.1186/s40001-024-02092-z.

[14] Ahsan MM, Luna SA, Siddique Z. Machine-learning-based disease diagnosis: a comprehensive review[J]. Healthcare, 2022, 10(3): 541. https://doi.org/10.3390/healthcare10030541.

[15] Huang C, Zhuo J, Liu C, et al. Development and validation of a diagnostic model to differentiate spinal tuberculosis from pyogenic spondylitis by combining multiple machine learning algorithms[J]. Biomol Biomed, 2024, 24(2): 401-410. https://doi.org/10.17305/bb.2023.9663.

[16] Shipe ME, Deppen SA, Farjah F, et al. Developing prediction models for clinical use using logistic regression: an overview [J]. J Thorac Dis, 2019, 11(Suppl 4): S574-S584. https://doi.org/10.21037/jtd.2019.01.25.

[17] Hong SH, Choi JY, Lee JW, et al. MR imaging assessment of the spine: infection or an imitation? [J]. RadioGraphics, 2009, 29(2): 599-612. https://doi.org/10.1148/rg.292085137.

[18] Zhang QC, Lu JJ, Ma YQ, et al. A diagnostic model for differentiating tuberculous spondylodiscitis from pyogenic spondylodiscitis based on pathogen-confirmed patients[J]. Eur Spine J, 2024, 33(12): 4664-4671. https://doi.org/10.1007/s00586-024-08433-0.

[19] Hu XJ, Zhang G, Zhang HQ, et al. A predictive model for early clinical diagnosis of spinal tuberculosis based on conventional laboratory indices: a multicenter real-world study[J]. Front Cell Infect Microbiol, 2023, 13: 1150632. https://doi.org/10.3389/fcimb.2023.1150632.

[20] Yan F, Chen X, Quan X, et al. Association between the stress hyperglycemia ratio and 28-day all-cause mortality in critically ill patients with sepsis: a retrospective cohort study and predictive model establishment based on machine learning[J]. Cardiovasc Diabetol, 2024, 23(1): 163. https://doi.org/10.1186/s12933-024-02265-4.

[21] Stoltzfus JC. Logistic regression: a brief primer[J]. Acad Emerg Med, 2011, 18(10): 1099-1104. https://doi.org/10.1111/j.1553-2712.2011.01185.x.

[22] O'Garra A, Redford PS, McNab FW, et al. The immune response in tuberculosis[J]. Annu Rev Immunol, 2013, 31: 475-527. https://doi.org/10.1146/annurev-immunol-032712-095939.

[23] Dyatlov AV, Apt AS, Linge IA. B lymphocytes in anti-mycobacterial immune responses: Pathogenesis or protection? [J]. Tuberculosis, 2019, 114: 1-8. https://doi.org/10.1016/j.tube.2018.10.011.

[24] Martineau AR, Wilkinson KA, Newton SM, et al. IFN-γ- and TNF-independent vitamin D-inducible human suppression of mycobacteria: the role of cathelicidin LL-37[J]. J Immunol, 2007, 178(11): 7190-7198. https://doi. org/10.4049/jimmunol.178.11.7190.

[25] Niki M, Yoshiyama T, Nagai H, et al. Nutritional status positively impacts humoral immunity against its *Mycobacterium tuberculosis*, disease progression, and vaccine development[J/OL]. PLoS One, 2020, 15(8): e0237062[2025-02-12]. https://doi.org/10.1371/journal.pone.0237062.

[26] Du ZX, Ren YY, Wang JL, et al. The potential association

©Journal of Central South University (Medical Science). All rights reserved.

between metabolic disorders and pulmonary tuberculosis: a Mendelian randomization study[J]. Eur J Med Res, 2024, 29 (1): 277. https://doi.org/10.1186/s40001-024-01845-0.

[27] Wu Q, Sheng Q, Michell D, et al. Anti-inflammatory effect of high-density lipoprotein blunted by delivery of altered microRNA cargo in patients with rheumatoid arthritis[J]. Arthritis Rheumatol, 2024, 76(5): 684-695. https://doi.org/10.1002/art.42782.

[28] Inoue M, Niki M, Ozeki Y, et al. High-density lipoprotein suppresses tumor necrosis factor alpha production by mycobacteria-infected human macrophages[J]. Sci Rep, 2018, 8 (1): 6736. https://doi.org/10.1038/s41598-018-24233-1.

[29] Lin PL, Flynn JL. CD8 T cells and *Mycobacterium tuberculosis* infection[J]. Semin Immunopathol, 2015, 37(3): 239-249. https://doi.org/10.1007/s00281-015-0490-8.

[30] Sanaei MJ, Nahid-Samiei M, Abadi MSS, et al. New insights into regulatory B cells biology in viral, bacterial, and parasitic infections[J]. Infect Genet Evol, 2021, 89: 104753. https://doi.org/10.1016/j.meegid.2021.104753.

[31] Grace PS, Peters JM, Sixsmith J, et al. Antibody-Fab and-Fc features promote *Mycobacterium tuberculosis* restriction[J]. bioRxiv, 2024: 2024.10.07.617070. https://doi.org/10.1101/2024. 10.07.617070.

[32] Huo Z, Yang M, Chen J, et al. Improved early diagnosis of difficult cases of tuberculous pleural effusion by combination of thoracoscopy with immunological tests[J]. Int J Infect Dis, 2019, 81: 38-42. https://doi.org/10.1016/j.ijid.2019.01.045.

[33] Wang G, Long J, Zhuang Y, et al. Application of metagenomic next-generation sequencing in the detection of pathogens in spinal infections[J]. Spine J, 2023, 23(6): 859-867. https://doi.org/10.1016/j.spinee.2023.02.001.

[34] Huang H, Shi J, Zheng M, et al. Pathogen detection in suspected spinal infection: metagenomic next-generation sequencing versus culture[J]. Eur Spine J, 2023, 32(12): 4220-4228. https://doi.org/10.1007/s00586-023-07707-3.

[35] Lv H, Liao S, Shi Z, et al. Application of metagenomic next-generation sequencing for rapid molecular identification in spinal infection diagnosis[J]. Front Cell Infect Microbiol, 2024, 14: 1382635. https://doi.org/10.3389/fcimb.2024.1382635.

[36] Gao Q, Liu Q, Zhang G, et al. Identification of pathogen composition in a Chinese population with iatrogenic and native vertebral osteomyelitis by using mNGS[J]. Ann Med, 2024, 56 (1): 2337738. https://doi.org/10.1080/07853890.2024.2337738.

[37] Li ZH, Zhang Q, Lian XF, et al. Value of metagenomic next-generation sequencing in the diagnosis of native pyogenic spinal infections: a multicenter, retrospective observational study[J]. Spine J, 2025, 25(4): 640-648. https://doi.org/10.1016/j.spinee.2024.11.004.

[38] Garg B, Mehta N, Mukherjee RN, et al. Epidemiological insights from 1, 652 patients with spinal tuberculosis managed at a single center: a retrospective review of 5-year data[J]. Asian Spine J, 2022, 16(2): 162-172. https://doi.org/10.31616/asj.2021.0137.

（责任编辑 宋柳）

©Journal of Central South University (Medical Science). All rights reserved.